

## Prediction of Reorganization Free Energies for Biological Electron Transfer: A Comparative Study of Ru-Modified Cytochromes and a 4-Helix Bundle Protein

Varomyalin Tipmanee,<sup>†,‡</sup> Harald Oberhofer,<sup>†</sup> Mina Park,<sup>§</sup> Kwang S. Kim,<sup>§</sup> and Jochen Blumberger<sup>\*,‡</sup>

*Department of Chemistry, University of Cambridge, Lensfield Road, Cambridge CB2 1EW, United Kingdom, Department of Physics and Astronomy, University College London, London WC1E 6BT, United Kingdom, and Center for Superfunctional Materials, Department of Chemistry, Pohang University of Science and Technology (POSTECH), San 31, Hyojadong, Namgu, Pohang (790-784), Korea*

Received September 1, 2010; E-mail: j.blumberger@ucl.ac.uk

**Abstract:** The acceleration of electron transfer (ET) rates in redox proteins relative to aqueous solutes can be attributed to the protein's ability to reduce the nuclear response or reorganization upon ET, while maintaining sufficiently high electronic coupling. Quantitative predictions of reorganization free energy remain a challenge, both experimentally and computationally. Using density functional calculations and molecular dynamics simulation with an electronically polarizable force field, we report reorganization free energies for intraprotein ET in four heme-containing ET proteins that differ in their protein fold, hydrophilicity, and solvent accessibility of the electron-accepting group. The reorganization free energies for ET from the heme cofactors of cytochrome *c* and *b*<sub>5</sub> to solvent exposed Ru-complexes docked to histidine residues at the surface of these proteins fall within a narrow range of 1.2–1.3 eV. Reorganization free energy is significantly lowered in a designed 4-helix bundle protein where both redox active cofactors are protected from the solvent. For all ET reactions investigated, the major components of reorganization are the solvent and the protein, with the solvent contributing close to or more than 50% of the total. In three out of four proteins, the protein reorganization free energy can be viewed as a collective effect including many residues, each of which contributing a small fraction. These results have important implications for the design of artificial electron transport proteins. They suggest that reorganization free energy may in general not be effectively controlled by single point mutations, but to a large extent by the degree of solvent exposure of the ionizable cofactors.

### 1. Introduction

The rate for long-range electron transfer (ET) in redox proteins can be several orders of magnitude larger than for the corresponding reaction in aqueous solution.<sup>1–3</sup> As an illustrative example, we consider ET between Fe<sup>2+</sup> and Fe<sup>3+</sup>. In aqueous solution, ET between the two ions occurs on the second time scale,<sup>4</sup> whereas when coordinated to the porphyrin groups of heme proteins, this reaction occurs on the microsecond–nanosecond time scale<sup>1–3</sup> over a distance that is about twice as large as in aqueous solution. This rate-accelerating effect is mainly based on the ability of the protein environment to minimize the molecular motions that lead to a degeneracy of the initial and final ET states and that facilitate resonant tunneling of the electron from the donor to acceptor group. Such molecular motions bridging the native configurations of initial and final

ET state include, for instance, the change in bond lengths of the oxidized and reduced cofactors and the reorientation of polar or charged protein residues and solvent molecules. The energy required for these motions to occur constitutes the activation barrier for long-range ET in proteins. It is the purpose of the present work to compute and characterize this barrier for pure electron tunneling reactions in heme containing proteins, to compare to available experimental data, and to gain insight into its molecular origin.

Experiments have shown that most<sup>1–3</sup> but not all<sup>5</sup> biological ET reactions are well described by semiclassical Marcus theory.<sup>6</sup> According to this theory, the rate is predicted to be proportional to the square of the electronic coupling matrix element,  $H_{12}$ , and an exponential term containing reorganization free energy,  $\lambda$ , and driving force,  $\Delta G$ :

$$k_c = \frac{2\pi}{\hbar} |H_{12}|^2 (4\pi\lambda k_B T)^{-1/2} \exp\left(-\frac{(\lambda + \Delta G)^2}{4\lambda k_B T}\right) \quad (1)$$

<sup>†</sup> University of Cambridge.

<sup>‡</sup> University College London.

<sup>§</sup> Pohang University of Science and Technology.

(1) Gray, H. B.; Winkler, J. R. *Q. Rev. Biophys.* **2003**, *36*, 341.

(2) Gray, H. B.; Winkler, J. R. *Chem. Phys. Lett.* **2009**, *483*, 1.

(3) Moser, C. C.; Keske, J. M.; Warncke, K.; Farid, R. S.; Dutton, P. L. *Nature* **1992**, *355*, 796.

(4) Sutin, N. In *Theory of Electron Transfer Reactions*; Zuckerman, J. J., Ed.; VCH: New York, 1986; Vol. 15, p 16.

(5) Wang, H.; Lin, S.; Allen, J. P.; Williams, J. C.; Blankert, S.; Laser, C.; Woodbury, N. W. *Science* **2007**, *316*, 747.

(6) Marcus, R. A.; Sutin, N. *Biochim. Biophys. Acta* **1985**, *811*, 265.

The latter two quantities define the activation free energy,  $\Delta G^\ddagger = (\lambda + \Delta G)^2/4\lambda$ . Thus, to understand the activation barrier of Marcus-like ET reactions, it is necessary to obtain reliable estimates for reorganization free energy and driving force. Experiments can give precise values for driving force and rate constants provided the ET reaction under consideration is amenable to measurements. Yet it is usually difficult to obtain direct and quantitative estimates for reorganization free energy from experiment.<sup>1,7</sup> Only a few experimentally determined estimates have been reported such as for intraprotein ET in Ru-modified azurin<sup>8</sup> and cytochrome,<sup>9,10</sup> primary charge separation in the photosynthetic bacterial reaction center,<sup>11</sup> and interprotein ET between two cytochrome proteins.<sup>12</sup> At the absence of experimental data, a generic value of 0.7 eV is often assumed.<sup>7</sup> Thus, in practice it is often unclear if a biological ET reaction is fast because the reorganization free energy is low or because the electronic coupling matrix element is particularly large. This issue is at the heart of an ongoing debate regarding the ET reaction between heme a and heme a<sub>3</sub> in the proton pump cytochrome *c* oxidase.<sup>7,13–15</sup>

Molecular dynamics simulation is a valuable alternative for estimation of reorganization free energy for biological ET.<sup>16–25</sup> Yet, calculations at a useful degree of accuracy (0.1 eV) are very challenging.<sup>16,24</sup> In previous work, we have computed the reorganization free energy for ET in a four-helix bundle protein that binds two porphyrin cofactors<sup>20</sup> (4-helix, see Figure 1) and in Ru(bpy)<sub>2</sub>(im)His33 cytochrome *c* (ccb) using a quantum mechanical-molecular mechanical (QM/MM) approach in combination with a nonpolarizable force field.<sup>24</sup> The value obtained for the four-helix bundle protein, 1.36 eV, was larger than the range of values expected on empirical grounds for proteins where both cofactors are excluded from the solvent (0.6–0.9 eV<sup>7</sup>). Similarly, for ccb we obtained a value of 1.61 eV from QM/MM as compared to the experimental value of 0.74 eV.<sup>10</sup> Preliminary investigations on ccb indicated that much of the

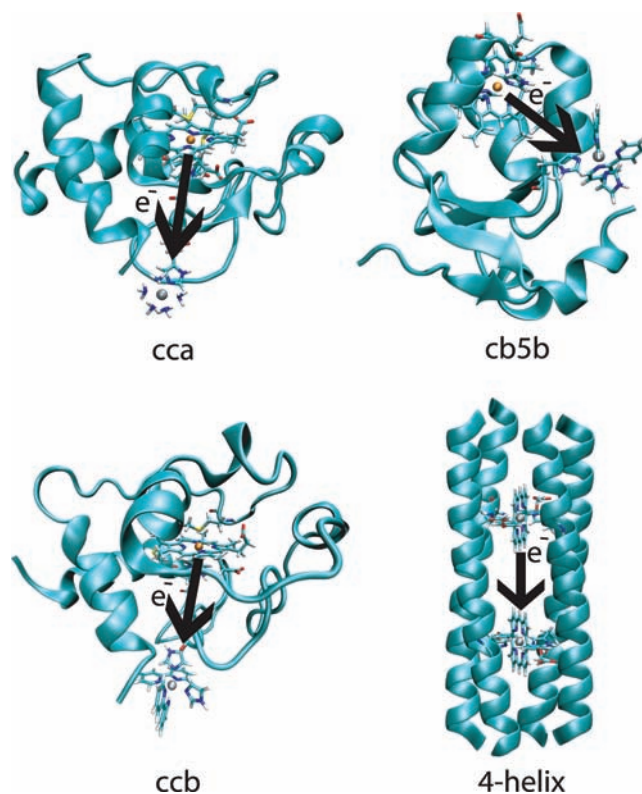


**Figure 1.** Simulated electron transfer proteins. Ru(am)<sub>5</sub>His33 cytochrome *c* (cca), Ru(bpy)<sub>2</sub>(im)His33 cytochrome *c* (ccb), Ru(bpy)<sub>2</sub>(im)His26 cytochrome *b*<sub>5</sub> (cb5b), and a designed four helix bundle protein that binds two Ru-diphenylporphyrin (RuDPP) cofactors (4-helix).<sup>20,30</sup> The structures were obtained as described in section 2. Arrows denote the transfer of an electron from the donor to the acceptor group. The protein is depicted in ribbon representation, and the redox active cofactors are shown in stick representation. Color code: H, white; C, green; N, blue; O, red; S, yellow; Fe, orange; Ru, silver. Solvent molecules are omitted.

- (7) Moser, C. C.; Page, C. C.; Dutton, P. L. *Philos. Trans. R. Soc., B* **2006**, *361*, 1295.
- (8) Di Bilio, A. J.; Hill, M. G.; Bonander, N.; Karlsson, B. G.; Villahermosa, R. M.; Malmström, B. G.; Winkler, J. R.; Gray, H. B. *J. Am. Chem. Soc.* **1997**, *119*, 9921.
- (9) Meade, T. J.; Gray, H. B.; Winkler, J. R. *J. Am. Chem. Soc.* **1989**, *111*, 4353.
- (10) Mines, G. A.; Bjerrum, M. J.; Hill, M. G.; Casimiro, D. R.; Chang, I.-J.; Winkler, J. R.; Gray, H. B. *J. Am. Chem. Soc.* **1996**, *118*, 1961.
- (11) Haffa, A. L. M.; Lin, S.; Katilius, E.; Williams, J. C.; Taguchi, A. K. W.; Allen, J. P.; Woodbury, N. W. *J. Phys. Chem. B* **2002**, *106*, 7376.
- (12) Kuila, D.; Baxter, W. W.; Natan, M. J.; Hoffman, B. M. *J. Phys. Chem. B* **1991**, *95*, 1.
- (13) Jasaitis, A.; Johansson, M. P.; Wikström, M.; Vos, M. H.; Verkhovsky, M. I. *Proc. Natl. Acad. Sci. U.S.A.* **2007**, *104*, 20811.
- (14) Beratan, D. N.; Balabin, I. A. *Proc. Natl. Acad. Sci. U.S.A.* **2008**, *105*, 403.
- (15) Kim, Y. C.; Wikstrom, M.; Hummer, G. *Proc. Natl. Acad. Sci. U.S.A.* **2009**, *106*, 13707.
- (16) Muegge, I.; Qi, P. X.; Wand, A. J.; Chu, Z. T.; Warshel, A. *J. Phys. Chem. B* **1997**, *101*, 825.
- (17) Ungar, L. W.; Newton, M. D.; Voth, G. A. *J. Phys. Chem. B* **1999**, *103*, 7367.
- (18) Simonson, T. *Proc. Natl. Acad. Sci. U.S.A.* **2002**, *99*, 6544.
- (19) Ceccarelli, M.; Marchi, M. *J. Phys. Chem. B* **2003**, *107*, 5630.
- (20) Blumberger, J.; Klein, M. L. *J. Am. Chem. Soc.* **2006**, *128*, 13854.
- (21) Cascella, M.; Magistrato, A.; Tavernelli, I.; Carloni, P.; Röthlisberger, U. *Proc. Natl. Acad. Sci. U.S.A.* **2006**, *103*, 19641.
- (22) Sulpizi, M.; Raugé, S.; VandeVondele, J.; Carloni, P.; Sprik, M. *J. Phys. Chem. B* **2007**, *111*, 3969.
- (23) Kerisit, S.; Rosso, K. M.; Dupuis, M.; Valiev, M. *J. Phys. Chem. C* **2007**, *111*, 11363.
- (24) Blumberger, J. *Phys. Chem. Chem. Phys.* **2008**, *10*, 5651.
- (25) LeBard, D. N.; Matyushov, D. V. *J. Phys. Chem. B* **2008**, *5218*, 112.

deviation with experiment is due to the missing electronic polarization of the outer-sphere medium.<sup>24</sup>

Previous experimental<sup>1,9,10,26,27</sup> and computational<sup>16,20,22</sup> works have shown that the major contribution to reorganization free energy is due to the protein and solvent (“outer” sphere), whereas the contribution due to the cofactors (“inner” sphere) is small. The role of the polypeptide in lowering the effective dielectric constant of the medium (and thus reorganization free energy) has been recognized, as well as the role of the solvent accessibility of the ionizable cofactor in tuning the outer-sphere reorganization.<sup>1</sup> However, there are a number of issues that are not well understood. For instance, it is not clear what the relative contributions of protein and solvent to reorganization free energy are. Experimental measurements on Ru-modified azurin in aqueous solution<sup>8</sup> and in protein crystals<sup>27</sup> gave similar reorganization free energy estimates, which led to the conclusion that solvent reorganization free energy is small, even though the electron acceptor was fully exposed to the solvent. On a molecular scale, it would be important to know whether reorganization free energy is a collective or a local effect, involving many amino acid residues or just a few, and what the actual protein motions are that give rise to the activation barrier. Such atomistic insight seems particularly relevant in

- (26) Amashukeli, X.; Gruhn, N. E.; Lichtenberger, D. L.; Winkler, J. R.; Gray, H. B. *J. Am. Chem. Soc.* **2004**, *126*, 15566.
- (27) Crane, B. R.; Di Bilio, A. J.; Winkler, J. R.; Gray, H. B. *J. Am. Chem. Soc.* **2001**, *123*, 11623.

view of possibilities to engineer proteins so as to optimize reorganization and activation free energy for biological electron tunnelling.

In this work, we report on electronically polarizable calculations for three Ru-modified proteins, Ru(am)<sub>5</sub>His33 cytochrome *c* (cca), Ru(bpy)<sub>2</sub>(im)His26 cytochrome *b*<sub>5</sub> (cb5b), and a designed 4-helix bundle protein (4-helix), that, together with our previously reported calculations for ccb, give in total four proteins that exhibit three different protein folds (see Figure 1). This choice allows us to investigate the effect of the protein fold, the hydrophilicity, and the solvent accessibility of the redox active cofactors on the reorganization free energy: in cca, the electron-accepting group is a hydrophilic, solvent-accessible Ru(am)<sub>5</sub> complex (am = NH<sub>3</sub>) docked to His33 at the surface of cytochrome *c*; in ccb, this complex is replaced by a hydrophobic but still solvent-accessible Ru(bpy)<sub>2</sub>(im) complex (bpy = bipyridine, im = imidazole); and in the 4-helix bundle, both cofactors are protected from the solvent.

We find that inclusion of electronic polarization via induced dipoles improves the agreement with experimentally determined reorganization free energy significantly. Proteins with one cofactor exposed to the solvent (cca, ccb, and cb5b) all fall within a narrow window of 1.2–1.3 eV, showing that this ET parameter is not very sensitive with respect to the different fold and the different hydrophilicity of the electron acceptor. However, placing both heme cofactors inside the scaffold of a designed 4-helix bundle protein, we predict that the reorganization is significantly lowered, by about 0.3 eV. The solvent contribution to reorganization is for all proteins, including the 4-helix bundle, close to or larger than 50%, showing that the dielectric response of the solvent is a major source for activation energy in the medium-sized proteins studied, even if the cofactors are solvent excluded. Finally, we find that in three out of the four ET systems studied, protein reorganization can be considered as a collective effect involving many residues, each contributing a small fraction.

## 2. Methods

The reorganization free energy for ET is calculated according to a QM+MM approach that was described in detail in ref 24. The total reorganization free energy,  $\lambda$ , is divided into the contribution of the ionizable cofactors and ligands,  $\lambda_i$  (subscript *i* for “inner sphere”), the contribution of the explicitly simulated protein and solvent,  $\lambda_o$  (subscript *o* for “outer sphere”), and a correction term accounting for the finite number of explicit solvent molecules,  $\lambda_{fs}$ .

$$\lambda = \lambda_i + \lambda_o + \lambda_{fs} \quad (2)$$

The assumption that inner- and outer-sphere contributions are additive was investigated previously for ccb by comparison to nonadditive QM/MM calculations.<sup>24</sup> In the latter, the QM energy optimization of the inner sphere is fully coupled to the electrostatic field of the protein. The QM/MM value for reorganization free energy differed by less than 0.1 eV from the QM+MM estimate, showing that the assumption of additivity gives sufficiently accurate results.

**Inner-Sphere Reorganization Energy.** The inner-sphere contribution is calculated for a gas-phase QM model of the donor and acceptor cofactors at the PBE/6-31++G(d,p)/PBE/6-31G(d) level of theory:

$$\lambda_i = \sum_{i=1,2} (E_{Ri}^* - E_{Ri} + E_{Oi}^* - E_{Oi})/2 \quad (3)$$

where  $E_{Ri}$  and  $E_{Oi}$  are the potential energies at the minimum energy configuration of cofactor *i* in the reduced (R) and oxidized state

(O), and  $E_{Ri}^*$  and  $E_{Oi}^*$  are the potential energies of states R and O at the minimum energy configuration of O and R, respectively. The sum in eq 3 is over donor (*i* = 1) and acceptor cofactor (*i* = 2). The electron acceptor of cca, Ru(am)<sub>5</sub>His33, was modeled as Ru(am)<sub>5</sub>(mim) (mim = methylimidazole) and the electron-donating cofactor of cb5b as Fe(porphin)(mim)<sub>2</sub>. Geometries were optimized at the PBE<sup>28</sup>/6-31G(d) level of theory using default convergence criteria. The final potential energies are calculated on the PBE/6-31G(d) geometries using the PBE functional and the 6-31++G(d,p) basis set for all atoms. The inner-sphere energies were found to be robust with respect to the exchange correlation functional used. The values obtained for PBE, BP, and B3LYP functionals were within 0.05 eV. All QM calculations were carried out with the Gaussian program package.<sup>29</sup> Inner-sphere reorganization energies for gas-phase models of the heme *c* cofactor of cca and ccb, of the electron-accepting cofactor of ccb and cb5b, Ru(bpy)<sub>2</sub>(im)His33/26, and of the Ru–diphenylporphyrin (RuDPP) cofactors of the 4-helix bundle were taken from refs 20, 24.

**Outer-Sphere Reorganization Energy.** The outer-sphere contribution is obtained from the thermal averages of the vertical energy gap  $\Delta E_o$  in the initial (A) and final diabatic states (B), that is, in the limit of linear response:

$$\lambda_o = (\langle \Delta E_o \rangle_A - \langle \Delta E_o \rangle_B)/2 \quad (4)$$

This approximation is rigorous when the fluctuations of the vertical energy gap  $\Delta E_o$  are Gaussian. In this case, the root-mean-square-deviation (rmsf) of the energy gap,  $\sigma_M = \langle \delta \Delta E_o^2 \rangle_M^{1/2}$ , in states A and B are equal, and eq 4 is equivalent with eq 5.

$$\lambda'_o = \frac{\sigma_A^2 + \sigma_B^2}{4k_B T} \quad (5)$$

The excess electron in states A and B is modeled as the difference in RESP atomic charges of the redox active cofactor in the reduced and oxidized states (see refs 20, 24). The outer-sphere energy gap is calculated according to eq 6:

$$\Delta E_o(\mathbf{R}^N) = E_B(\mathbf{R}^N) - E_A(\mathbf{R}^N) - (IE_1(\mathbf{R}^N) - IE_2(\mathbf{R}^N)) \quad (6)$$

$$IE_i(\mathbf{R}^N) = \sum_{j \neq k \in \text{QM}_i} \frac{q_{j,O} q_{k,O} - q_{j,R} q_{k,R}}{R_{jk}} \quad (7)$$

where  $E_A(\mathbf{R}^N)$  and  $E_B(\mathbf{R}^N)$  denote the total electrostatic potential energy in states A and B at a configuration  $\mathbf{R}^N$ .  $IE_i$  is the self-contribution of cofactor *i* to  $E_B - E_A$ , comprised of the electrostatic interaction between all ionizable atoms *j* of cofactor *i*, denoted QM<sub>*i*</sub> atoms, with charge  $q_{j,O}$  and  $q_{j,R}$  in states O and R, respectively. The self-contribution is subtracted as it is taken into account in the QM calculations, eq 3.

Molecular dynamics simulations were carried out for calculation of the thermal averages of  $\Delta E_o$  for aqueous solutions of cca, cb5b, and the 4-helix bundle protein, respectively. Simulation data for ccb were taken from ref 24. In cca, the electron-accepting Ru-complex is composed of polar ammonia ligands that can form hydrogen bonds with the nearby charged residues Glu104 and Lys22. To improve the sampling of the slow hydrogen-bond dynamics, we have calculated two independent trajectories starting from different NMR structures of the protein. The initial structures

(28) Perdew, J. P.; Burke, K.; Ernzerhof, M. *Phys. Rev. Lett.* **1996**, *77*, 3865.

(29) Frisch, M. J.; et al. *Gaussian 03*, revision C.01; Gaussian, Inc.: Wallingford, CT, 2004.

(30) Cochran, F. V.; Wu, S. P.; Wang, W.; Nanda, V.; Saven, J. G.; Therien, M. J.; DeGrado, W. F. *J. Am. Chem. Soc.* **2005**, *127*, 1346.



were generated by docking the Ru(am)<sub>5</sub> complex to His33 of cytochrome *c* using the NMR structures 40 and 3 as reported in the pdb file 2GIW. Structure 3 has the largest rmsd of all 40 structures reported in the pdb file relative to structure 40. The trajectory initiated from structure 40 is denoted trajectory 1, and the one initiated from structure 3 is denoted trajectory 2. For cb5b, the Ru(bpy)<sub>2</sub>(im) complex was docked to His26 of cytochrome *b*<sub>5</sub> using the crystal structure 1CYO. The starting structure for the 4-helix bundle protein was a snapshot from a previous MD simulation,<sup>20</sup> which was initiated from a model structure.<sup>30</sup> The protonation state for cca and ccb was adopted from the NMR structure 2GIW (that included proton positions), and the protonation states of the ionizable residues of cb5b and 4-helix were modeled at pH = 7.

The simulation protocol is similar to our previous study.<sup>24</sup> The solvated protein solutions were equilibrated at 300 K and 1 bar with the nonpolarizable AMBER99 force field and TIP3P water for about 10 ns. After further equilibration with the polarizable AMBER02 force field and POL3 water for about 2 ns in the NPT ensemble, the following 8 ns of dynamics was taken for calculation of thermal averages. The integration time step was 1 fs for the polarizable calculations and 2 fs for the nonpolarizable calculations.  $\lambda_o$  was obtained according to eq 4, by calculation of the outer-sphere gap energy eq 6 for 800 equidistantly spaced configurations using the AMBER02 force field and POL3 water. For cca, the average of trajectories 1 and 2 is reported. The MD simulations and energy gap calculations were carried out in periodic boundary conditions using Ewald summation for calculation of the electrostatic (charge + dipolar) interactions. The molecular dynamics calculations were carried with the NAMD<sup>31</sup> and AMBER9 simulation packages.<sup>32</sup>

**Bulk Solvent Reorganization Energy.** The most rigorous way to estimate the missing contribution due to bulk solvent is to carry out simulations of the solute for a varying number of solvent molecules and extrapolate the results to the infinite dilution limit. However, this is impractical for solutes as large as proteins. Here, we calculate the finite size correction for a model ET reaction, the aqueous Ru<sup>2+</sup>(H<sub>2</sub>O)<sub>6</sub>–Ru<sup>3+</sup>(H<sub>2</sub>O)<sub>6</sub> electron self-exchange reaction, at unit cell dimensions and donor–acceptor distance that are the same as in the ET proteins. This value is then adopted as a finite size correction for the ET proteins. We note that the correction is due to water molecules that are more than 30 Å away from the redox active sites. Thus, their atomistic details should be less relevant. The reorganization free energy for Ru<sup>2+</sup>(H<sub>2</sub>O)<sub>6</sub>–Ru<sup>3+</sup>(H<sub>2</sub>O)<sub>6</sub> electron self-exchange is computed for systems containing 1115, 2604, 5166, 8709, and 13633 TIP3P water molecules (including the 12 first shell water molecules). The molecular model and the simulation protocol are the same as in our previous study.<sup>33</sup> The only difference is that the Ru–Ru distance was chosen to be 18 Å, which is the average donor–acceptor distance in the four ET proteins studied. The reorganization free energy due to the solvent (excluding the 12 first shell water molecules) is shown in Figure 2 as a function of the inverse volume of the unit cell, ( $V^{-1} = L^{-3}$ ). The  $R^2$  value of the linear fit is 0.998. The average inverse volume of the unit cell used for the protein simulations is indicated by a red cross in Figure 2. The difference in reorganization free energy at this point and the intercept (the infinite dilution limit) is  $\lambda_{fs} = 0.06$  eV. We note that a similar finite size correction was used in ref 20 on the basis of continuum electrostatics calculations.

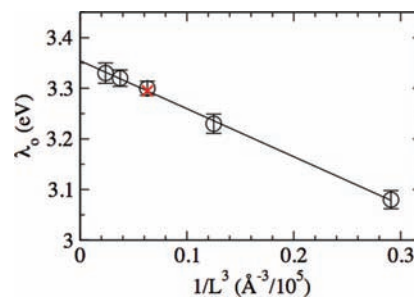


**Figure 2.** Outer-sphere reorganization free energy for electron transfer in an aqueous model system as a function of the inverse volume of the unit cell ( $L$  = box length). The reorganization free energy at a system size used in present protein simulations is denoted by a cross. Statistical errors due to the finite length of the MD runs are indicated. See section 2 for details.

**Nuclear Quantum Effects.** For calculation of nuclear quantum effects, we have adopted the quantized rate equation for a harmonic (Spin-Boson) model.<sup>35</sup>

$$k_q = \frac{2\pi}{\hbar} |H_{12}|^2 \frac{\beta}{2\pi} \int_{-\infty}^{\infty} dR \exp\left[-(\beta/2 + i\beta R)\Delta G - \frac{2}{\pi\hbar} \int_0^{\infty} d\omega \frac{J(\omega) \cosh(\beta\hbar\omega/2) - \cosh(iR\beta\hbar\omega)}{\omega^2 \sinh(\beta\hbar\omega/2)}\right] \quad (8)$$

The spectral density function  $J(\omega) = \beta\omega/2 \int_0^{\infty} dt (\delta\Delta E(0)\delta\Delta E(t))_A \cos \omega t$  was obtained from molecular dynamics simulation by calculating the full ET energy  $\Delta E = E_B - E_A$  every 4 fs along a 100 ps trajectory. The nonpolarizable Amber99 force field and TIP3P water were used for this purpose because TIP3P water gave better results than POL3 water for the quantum corrections for Ru<sup>2+</sup>–Ru<sup>3+</sup> electron self-exchange.<sup>33</sup> The quantum enhancement factor  $k_q/k_c$  was then obtained as the ratio of eqs 8 and 1 using the reorganization free energy defined in terms of  $J(\omega)$ ,  $\lambda = 2/\pi \int_0^{\infty} d\omega J(\omega)/\omega$ , for evaluation of eq 1.  $\Delta G$  was taken from experiment.<sup>9,10,36</sup>

**Oxidation of Heme c in ccb.** Reorganization energy calculations were also carried out for oxidation of heme c in ccb (discussed in section 4). The initial diabatic state A is the same as for ET; that is, the heme group is in the reduced state and the Ru-complex in the oxidized state (Fe<sup>2+</sup>–Ru<sup>3+</sup>). In the final diabatic state B, only the heme group changes oxidation state (Fe<sup>3+</sup>–Ru<sup>3+</sup>). The inner-sphere contribution eq 3 is due to the heme c cofactor, only,  $\lambda_i = 0.03$  eV. The outer-sphere energy gap is calculated according to eq 6, noting that  $E_B$  is now the energy of Fe<sup>3+</sup>–Ru<sup>3+</sup> and that  $IE_2$  is equal to zero. Molecular dynamics simulations in states A and B are carried out using the same system composition and force field parameter as for ET and following the same simulation protocol, giving  $\lambda_o = 0.48$  eV. For estimation of finite size effects, we have taken the  $1/L$  extrapolation data of Ru<sup>2+</sup>(bpy)<sub>3</sub> in POL3 water as reported in ref 34 ( $R^2 = 0.991$ ). The difference in reorganization free energy at the inverse box length used in present protein simulations, and at the intercept of the  $1/L$  extrapolation, is  $\lambda_{fs} = 0.20$  eV. This is slightly larger than our previous estimate of 0.12 eV based on continuum electrostatics calculations.<sup>20</sup> Summing up all three terms, the total outer-sphere reorganization free energy for heme c oxidation is estimated to be  $\lambda = 0.71$  eV.

### 3. Results

**Energy Gap Fluctuations.** The central quantity in the present investigation is the vertical energy gap, which is the energy required to transfer an electron from the donor to the acceptor group at fixed nuclear configuration. The thermal fluctuations

(31) Phillips, J. C.; Braun, R.; Wang, W.; Gumbart, J.; Tajkhorshid, E.; Villa, E.; Chipot, C.; Skeel, R. D.; Kale, L.; Schulten, K. *J. Comput. Chem.* **2005**, *26*, 1781.

(32) Case, D. A.; et al. *AMBER 9*; University of California: San Francisco, CA, 2006.

(33) Blumberger, J.; Lamoureux, G. *Mol. Phys.* **2008**, *106*, 1597.

(34) Seidel, R.; Faubel, M.; Winter, B.; Blumberger, J. *J. Am. Chem. Soc.* **2009**, *131*, 16127.

(35) Song, X.; Marcus, R. A. *J. Chem. Phys.* **1993**, *99*, 7768.

(36) Jacobs, B. A.; Mauk, M. R.; Funk, W. D.; MacGillivray, R. T. A.; Mauk, A. G.; Gray, H. B. *J. Am. Chem. Soc.* **1991**, *113*, 4390.

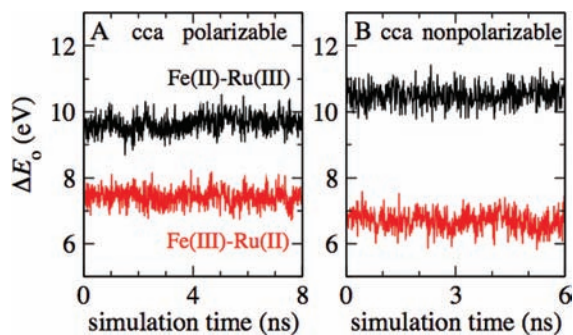


**Figure 3.** Fluctuations of the outer-sphere energy gap  $\Delta E_o$  (eq 6) along molecular dynamics trajectories of cca in the initial state (black) and final state (red). In panel (A) a polarizable force field is used (trajectory 1) and in panel (B) a nonpolarizable force field is used.

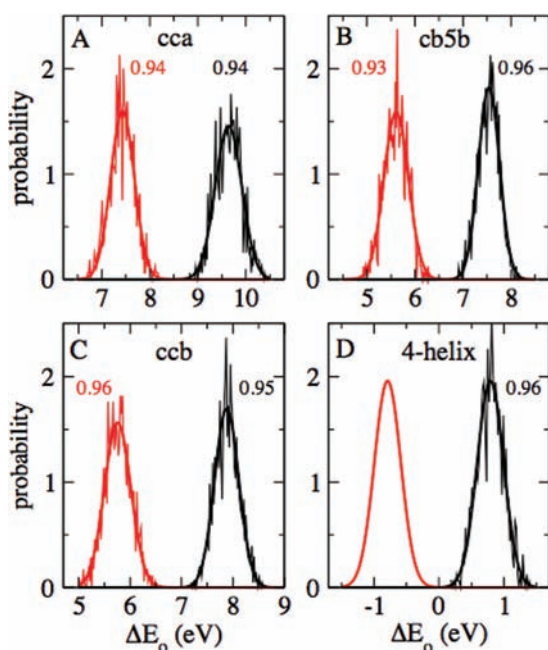


**Figure 4.** Probability distribution of the outer-sphere energy gap  $\Delta E_o$  (eq 6) for the 4 ET proteins shown in Figure 1. The distributions shown in black are for the initial state ( $\text{Fe}^{2+}-\text{Ru}^{3+}$ ), and the ones shown in red are for the final state ( $\text{Fe}^{3+}-\text{Ru}^{2+}$ ). Data points within two standard deviations of the average energy gap were collected in bins of width 0.02 eV (thin lines). Gaussian fit functions are shown in thick lines, and the corresponding correlation coefficients are indicated. The distributions for the 4-helix bundle are symmetric (electron self-exchange), and the distribution corresponding to trajectory 1 is shown for cca.

of the electrostatic contribution of the protein and solvent to the energy gap,  $\Delta E_o$  of eq 6 (“o” for outer sphere), are shown for cca in Figure 3A. The fluctuations were obtained from multianosecond molecular dynamics trajectories in the initial and final ET states, respectively. Sampling on this time scale is sufficient to converge the average to a statistical uncertainty of 0.03 eV. The probability distributions corresponding to the fluctuations of the energy gaps are shown in Figure 4. They are well approximated by Gaussian distributions for all four proteins, fitting the simulated data with correlation coefficients of 0.94–0.96. The Gaussian nature of the fluctuations and the fact that the root-mean-square fluctuations (rmsf) in the initial ET state,  $M = A$ , differs by not more than 0.02 eV from the fluctuations in the final ET state,  $M = B$ , indicate that the four ET proteins are well described in the linear response approxima-

**Table 1.** Summary of Electron Transfer Properties Obtained from Molecular Dynamics Simulation of the Proteins Shown in Figure 1<sup>a</sup>

	cca <sup>b</sup>	ccb	cb5b	4-helix
$\langle \Delta E_o \rangle_A^c$	9.81 ± 0.03	7.88 ± 0.02	7.53 ± 0.01	0.79 ± 0.02
$\langle \Delta E_o \rangle_B^c$	7.46 ± 0.01	5.76 ± 0.03	5.60 ± 0.02	
$\langle \delta \Delta E_o^2 \rangle_A^{1/2 d}$	0.26 ± 0.01	0.24 ± 0.01	0.22 ± 0.01	0.21 ± 0.01
$\langle \delta \Delta E_o^2 \rangle_B^{1/2 d}$	0.25 ± 0.01	0.25 ± 0.01	0.24 ± 0.00	
$\lambda_o^e$	1.17 ± 0.02	1.06 ± 0.02	0.97 ± 0.01	0.79 ± 0.02
$\lambda_o^f$	1.28 ± 0.04	1.15 ± 0.05	1.03 ± 0.03	0.84 ± 0.05
$\lambda_{is}^g$	0.06	0.06	0.06	0.06
$\lambda_i^h$	0.11	0.14	0.14	0.09
$\lambda^i$	1.34 ± 0.02	1.26 ± 0.02	1.17 ± 0.01	0.94 ± 0.02
$\lambda$ (exp)	1.15–1.24 <sup>j</sup>	0.74 <sup>k</sup>		
$k_q/k_c^l$	3.7	1.7	1.1	1.5

<sup>a</sup> All energies are in eV. <sup>b</sup> Average of trajectories 1 and 2. <sup>c</sup> Equation 6. Statistical error =  $(s/N)^{1/2} \langle \delta \Delta E_o^2 \rangle_M^{1/2}$ , where  $s$  is the statistical inefficiency, and  $N$  the number of data points.  $\langle \Delta E_o \rangle_B = -\langle \Delta E_o \rangle_A$  for the 4-helix bundle protein (electron self-exchange). <sup>d</sup> Root-mean-square fluctuations (rmsf) of  $\Delta E_o$ . Statistical error is the standard deviation of the rmsf calculated for blocks of the trajectory of length 20s.  $\langle \delta \Delta E_o^2 \rangle_B^{1/2} = \langle \delta \Delta E_o^2 \rangle_A^{1/2}$  for the 4-helix bundle protein. <sup>e</sup> Outer-sphere reorganization free energy, eq 4. <sup>f</sup> Outer-sphere reorganization free energy, eq 5. <sup>g</sup> Finite size correction to  $\lambda_o$ . <sup>h</sup> Inner-sphere reorganization free energy, eq 3. <sup>i</sup> Total reorganization free energy, eq 2. Statistical error is due to finite sampling of  $\Delta E_o$ . <sup>j</sup> Experimental reorganization free energy, ref 9. <sup>k</sup> Experimental reorganization free energy, ref 10. <sup>l</sup> Nuclear quantum enhancement factor, eqs 1 and 8.

tion. This is in agreement with our previous work on the 4-helix bundle protein<sup>20</sup> and with the results for oxidation of cytochrome *c*.<sup>18</sup>

**Reorganization Energies.** Adopting the linear response formula eq 4, we obtain outer-sphere reorganization free energies ranging from  $\lambda_o = 0.79$  eV for the 4-helix bundle to 1.17 eV for cca (average of trajectory 1 (1.11 eV) and trajectory 2 (1.24 eV)). Using the alternative definition for reorganization free energy eq 5, these values are reproduced to within 0.1 eV (see Table 1 for a summary). Indeed, eqs 5 and 4 are equivalent in the limit of Gaussian statistics. This is a further indication that the protein ET is fairly well described in the linear response approximation and that the Marcus picture of two crossing parabolas applies. As the statistical error for the average energy gap is smaller than for the rmsf, we prefer to base our subsequent analysis and discussion on  $\lambda_o$  rather than  $\lambda_o'$ .

The outer-sphere reorganization free energy obtained from simulation includes the reorganization of the protein and of about 5000 water molecules, but excludes the reorganization of the bulk solvent. The latter is estimated to be 0.06 eV, as described in section 2, increasing the total outer-sphere contribution of cca to  $1.17 + 0.06 = 1.23$  eV. The inner-sphere contribution obtained from density functional theory calculations for gas-phase models of heme *c* and the Ru-complex is  $\lambda_i = 0.11$  eV. Thus, the total reorganization free energy for ET from heme *c* to the Ru-complex is  $\lambda = 1.34$  eV. This is close to the experimental range of 1.15–1.24 eV obtained from the driving force dependence of the ET rate for charge separation and recombination in Zn–heme cca.<sup>9</sup> We would like to emphasize that the good agreement with experiment was achieved by using a polarizable force field for the protein (Amber02<sup>32</sup>) and a polarizable water model (POL3<sup>37</sup>). For the nonpolarizable model (Amber99<sup>32</sup> and TIP3P water<sup>38</sup>), the reorganization free energy is overestimated by 40% as can be seen from the too large gap

(37) Caldwell, J. W.; Kollman, P. A. *J. Phys. Chem.* **1995**, *99*, 6208.

(38) Jorgensen, W. L.; Chandrasekhar, J.; Madura, J. D.; Impey, R. W.; Klein, M. L. *J. Chem. Phys.* **1983**, *79*, 926.

between the ET energy in initial and final states in Figure 3 (B). A similar overestimation is observed for the other three proteins.

The total reorganization free energies of cca, ccb, and cb5b are remarkably similar and fall within a range of 0.2 eV (see Table 1). The value for ccb, 1.26 eV, is slightly larger than our previous estimate, which did not include a finite size correction.<sup>24</sup> A common feature of cca, ccb, and cb5b is that the electron-accepting Ru-complex is docked to a residue at the surface of the protein, thus being fully exposed to the solvent; see Figure 1. In contrast, both cofactors of the designed 4-helix bundle are located in the interior of the protein and are less solvent accessible. Interestingly, the reorganization free energy for the 4-helix bundle is significantly smaller than those for the three cytochrome proteins. The difference, about 0.3 eV, corresponds to a significant enhancement in the ET rate, a factor of 18 at zero driving force. We note that the absolute value of  $\lambda$  for the 4-helix bundle is smaller than in our previous investigation,<sup>20</sup> mainly because an improved force field with explicit electronic polarization was used in the present study.

**Nuclear Quantum Effects.** The semiclassical rate expression eq 1 is exact within the harmonic approximation in the limit  $k_B T \gg \hbar\omega_i$ , where  $\omega_i$  denote the frequencies of the molecular motions that couple to electron transfer. For large frequencies or low temperature, nuclear quantum effects become important. For their estimation, we have adopted a harmonic (Spin-Boson) model<sup>35</sup> with the quantized rate constant given in eq 8, and we calculated the spectral density function  $J(\omega)$  for the four ET proteins from molecular dynamics simulation. The resultant quantum enhancement factor  $k_q/k_c$ , which is the ratio of quantum and classical rate constant given by eqs 8 and 1, respectively, is summarized in Table 1. The values range from 1.1 for cb5b to 3.7 for cca, indicating that nuclear quantum effects are small for these proteins at room temperature. We have further attempted to calculate a single effective frequency by inserting the Franck–Condon factor of  $k_q$  into the quantized rate expression for a single effective mode coupling to ET:<sup>39,40</sup>

$$k'_q = \frac{2\pi}{\hbar} |H_{12}|^2 \text{FC}$$

$$\text{FC} = \frac{1}{\hbar\omega} (n + 1/n)^{P/2} I_P(2S(n(n+1))^{1/2}) \exp[-S(2n+1)] \quad (9)$$

In eq 9,  $S = \lambda/\hbar\omega$ ,  $P = -\Delta G/\hbar\omega$ ,  $n = [\exp(\hbar\omega/k_B T) - 1]^{-1}$ , and  $I_P$  is the modified Bessel function of the first kind of order  $P$ . We have attempted to obtain an effective frequency by evaluating the right-hand side of eq 9 for a range of values for  $\omega$  and matching the Franck–Condon factor (FC) of  $k'_q$  with the FC factor of  $k_q$ . The latter contains all frequencies sampled with molecular dynamics simulation. For cca and 4-helix, we obtained an effective frequency  $\omega$  of about 470 cm<sup>-1</sup> (60 meV) and 290 cm<sup>-1</sup> (40 meV), respectively; for ccb the solution was not unique (nine frequencies between 560–1520 cm<sup>-1</sup>), and for cb5b we did not obtain a solution. The frequency for cca is close to the value considered adequate for a wide range of intraprotein ET reactions, 70 meV (560 cm<sup>-1</sup>).<sup>41</sup> However, the error in the frequency determined this way is rather large because of the exponential dependence in the FC factor of eq 8. For instance,

if the FC factor obtained from molecular dynamics simulation is doubled or reduced to a half, the effective frequency shifts by more than 200 cm<sup>-1</sup>.

#### 4. Discussion

**Comparison to Experiment.** The agreement between computed and experimental reorganization free energy in cca is fairly good for the polarizable force field; the deviation is no more than the experimental uncertainty of 0.1 eV. Interestingly, the nonpolarizable force field gives values that are systematically overestimated by about 40%. The need for inclusion of explicit electronic polarizability in ET simulations has been repeatedly pointed out in the literature<sup>17,19,24,33,42,43</sup> and can be explained by a continuum model for reorganization. The reorganization free energy is predicted to be proportional to the Pekar factor of the medium,  $1/\epsilon_{op} - 1/\epsilon_s$ , where  $\epsilon_{op}$  and  $\epsilon_s$  are the optical and static dielectric constants, respectively. The experimental optical dielectric constant of cca in 0.1 M NaCl can be estimated to be  $\epsilon_{op} = 1.84$  (based on the refractive index measured for hen egg white lysozyme solutions as explained in ref 24), but  $\epsilon_{op} = 1$  for nonpolarizable force field models. Thus, assuming that  $\epsilon_s \gg \epsilon_{op}$ , the reorganization free energy is predicted to be overestimated by about 45%. The smaller overestimation obtained from molecular dynamics simulation (32% for ccb, 37% for cb5b, 40% for cca, 41% for 4-helix) confirms the view that the continuum model predicts a too strong dependence of reorganization on the optical dielectric constant.<sup>33,44</sup> However, the polarizable water model used (POL3<sup>37</sup>) has the tendency to slightly underestimate electronic polarization effects,<sup>45</sup> which could also explain the small remaining deviation between computed and experimental values for cca.

Going from cca to ccb, experiments predict a substantial decrease in reorganization free energy, from 1.15–1.24 eV<sup>9</sup> to 0.74 eV,<sup>10</sup> whereas our computations predict a smaller decrease from 1.34 to 1.26 eV, respectively. There are a few indications that lend support to the computed values. First, we note that in ccb the reorganization free energy is dominated by the contribution of the solvent (see below), 0.93 eV or 79% of the total 1.26 eV, and most of the solvent reorganization occurs in the vicinity of the Ru(bpy)<sub>2</sub>(im)His33 complex. Thus, if the calculations overestimate reorganization free energy, the reason for it should be related to the limited accuracy of the solvent model used and its interactions with the Ru(bpy)<sub>2</sub>(im)His33 complex. Previous work suggests that this is not the case, however. The POL3 water model employed here was very successfully used for the computation of reorganization free energy for oxidation of aqueous Ru(bpy)<sub>3</sub><sup>2+/3+</sup><sup>34</sup> and other ions in aqueous solution; see Table 2. The bpy-complex has solvation properties that are very similar to the ones of the electron acceptor Ru(bpy)<sub>2</sub>(im)His33 of ccb. The experimental value obtained from photoemission spectroscopy could be reproduced with our QM+MM(POL3) calculations to within 0.1 eV.<sup>34</sup> Similarly, higher level computations of reorganization free energy, where solute and solvent were simulated using density functional molecular dynamics (DFMD), could be reproduced with the QM+MM approach to within 0.1 eV.<sup>34</sup> This strongly suggests that the POL3 water model used in the present

(39) Jortner, J. *J. Chem. Phys.* **1976**, *64*, 4860.

(40) Jasaitis, A.; Rappaport, F.; Pilet, E.; Liebl, U.; Vos, M. H. *Proc. Natl. Acad. Sci. U.S.A.* **2005**, *102*, 10882.

(41) Page, C. C.; Moser, C. C.; Chen, X.; Dutton, P. L. *Nature* **1999**, *402*, 47.

(42) King, G.; Warshel, A. *J. Chem. Phys.* **1990**, *93*, 8682.

(43) Sterpone, F.; Ceccarelli, M.; Marchi, M. *J. Phys. Chem. B* **2003**, *107*, 11208.

(44) Gupta, S.; Matyushov, D. V. *J. Phys. Chem. A* **2004**, *108*, 2087.

(45) Ren, P.; Ponder, J. W. *J. Phys. Chem. B* **2003**, *107*, 5933.



**Table 2.** Summary of Previous Calculations of Reorganization Free Energy, Where the POL3 Water Model Was Employed in QM+MM Calculations<sup>a</sup>

reaction (aqueous solution)	$\lambda$ (QM+MM)	$\lambda$ (DFMD)	$\lambda$ (exp)
$\text{Ru}(\text{bpy})_3^{2+} \rightarrow \text{Ru}(\text{bpy})_3^{3+} + \text{e}^-$ <sup>b</sup>	1.24	1.20	1.21
$\text{Mn}^{2+} \rightarrow \text{Mn}^{3+} + \text{e}^-$ <sup>c</sup>	3.09	3.19	2.98
$\text{Ru}^{2+} + \text{Ru}^{3+} \rightarrow \text{Ru}^{3+} + \text{Ru}^{2+}$ <sup>d</sup>	1.78		1.7–1.8

<sup>a</sup> DFMD stands for (all QM) density functional molecular dynamics and exp for experiment. <sup>b</sup> QM+MM value reported in the Supporting Information of ref 34. <sup>c</sup> Reference 48. QM+MM value is the sum of the inner-sphere contribution ( $\lambda_i = 1.01$  eV<sup>48</sup>) and the outer-sphere contribution, reported for Ru–hexahydrate in the Supporting Information of ref 34 ( $\lambda_{\infty}^{\text{out}} = 2.08$  eV). <sup>d</sup> Reference 49. QM+MM value for 5 M ionic strength and a Ru–Ru separation distance of 5.5 Å. Exp. denotes the range of values for which the computed rate<sup>49</sup> reproduces the experimental rate.<sup>50</sup>

QM+MM calculations does not overestimate the solvent reorganization, despite the fact that electronic polarizability is somewhat underestimated in this water model.<sup>45</sup> Second, as a further test of the QM+MM approach, we have calculated the reorganization free energy for heme one-electron oxidation of ccb (see section 2) and obtain a value of 0.71 eV, in fairly good agreement with the experimental value for horse-heart cytochrome *c* as obtained from electrochemical measurements, 0.58 eV.<sup>46</sup> The small overestimation could be due to the fact that in experiment the protein resides in the vicinity of the electrode and is thus not fully solvated. Third, while in ref 10 a commendable effort was made to obtain data points for large driving forces, only one data point in the inverted region is reported. This makes the fit to an inverted parabola and the estimation of  $\lambda$  from the position of the maximum of the inverted parabola statistically somewhat uncertain. Clearly, to resolve the discrepancy between experiment and simulation, it would be highly desirable if the measurements could be extended to include more data points in the inverted region.

**Analysis of Reorganization Free Energy Contributions.** The individual contributions of the redox active cofactors, solvent, and protein to the reorganization free energy are shown in Figure 5. The cofactor contributions obtained from density functional calculations are small ranging from  $\lambda_i = 0.09$  eV for the 4-helix bundle<sup>20</sup> to 0.11–0.14 eV for the cytochrome proteins. This is in quantitative agreement with experimental data. Using photoelectron spectroscopy, a value  $\lambda_i = 0.12$ –0.14 eV was obtained for ET in a Zn-porphin dimer,<sup>26</sup> while for one-electron oxidation of  $\text{Ru}(\text{am})_2^{2+}$   $\lambda_i \approx 0.05$  eV was estimated.<sup>47</sup> Neglecting the small difference between Zn-porphin and the heme *c* cofactor in *cca*, the estimate based on experimental data,  $0.14/2 + 0.05 = 0.12$  eV, is virtually identical to our computed value of 0.11 eV. The inner-sphere reorganization thus contributes only about 10% to the total reorganization free energy.

The major sources for reorganization free energy are the protein and the solvent. To distinguish between these two contributions, we recalculated the energy gap for the same ensemble of protein configurations that was used in the calculation of the total energy gap, but now with all water molecules, ions, and periodic images removed from the system.

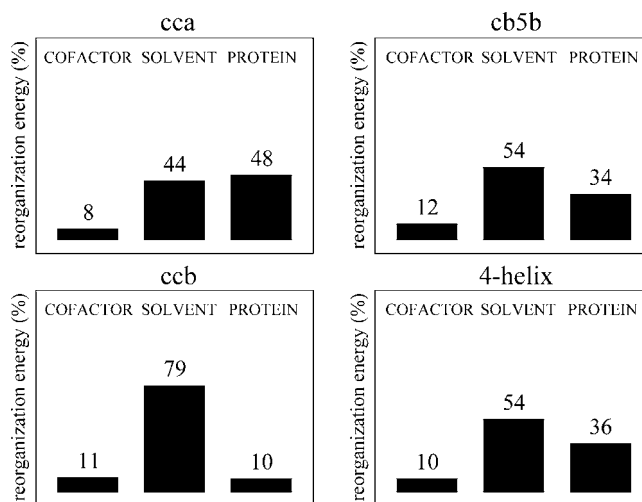


**Figure 5.** Contribution of the cofactors, solvent, and protein to reorganization free energy in percent (%) of the total value. For *cca*, the average of trajectories 1 and 2 is given. See section 4 for a discussion.

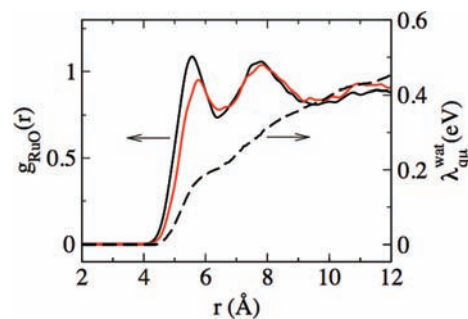


**Figure 6.** Radial distribution function between the Ru atom of the  $\text{Ru}(\text{bpy})_2\text{imHis33}$  complex of *ccb* and the oxygen atoms of water molecules,  $g_{\text{RuO}}(r)$ . The distribution for the initial state ( $\text{Ru}^{3+}$ ) is shown in black solid lines, and the distribution for the final state ( $\text{Ru}^{2+}$ ) is shown in red solid lines. The distributions were smoothed by convolution with a Gaussian of width 0.1 Å. Reorganization free energy of water molecules as a function of distance to the Ru-complex is shown in dashed lines.  $\lambda_{\text{qm}}^{\text{wat}}(r)$  is the reorganization free energy of all water molecules contained in a sphere of radius  $r$  that is centered at the center of mass of the Ru-complex.  $\lambda_{\text{qm}}^{\text{wat}}(r)$  consists of the fixed charge contribution to reorganization free energy, only (induced dipole contribution is omitted).

The difference between total reorganization free energy (computed in periodic boundary conditions) and the protein contribution (isolated system) is then generally referred to as the solvent contribution (water+ions+periodic images). As can be seen in Figure 5, the solvent contributions are in general larger than the protein contributions. In *cca*, *ccb*, and *cb5b*, most of the solvent contribution is due to the water molecules solvating the electron accepting Ru-complex. This is illustrated in Figure 6, where we show the radial distribution of the Ru atom and O atoms of the water molecules for the initial and final state of *ccb*. Upon electron injection into the Ru-complex, the first maximum of the radial distribution is shifted to larger distances as a consequence of the repulsive interaction between the electron and the water dipoles. The solvent contribution of the 4-helix bundle protein is mainly associated with reorganization of water molecules that temporarily penetrate the empty space between the two cofactors. While this effect is the dominant outer-sphere contribution in the 4-helix bundle protein, it is significantly smaller in absolute terms than the solvent reorganization in the other three proteins.

(46) Terrettaz, S.; Cheng, J.; Miller, C. J.; Guiles, R. D. *J. Am. Chem. Soc.* **1996**, *118*, 7857.

(47) Siders, P.; Marcus, R. A. *J. Am. Chem. Soc.* **1981**, *103*, 741.

(48) Moens, J.; Seidel, R.; Geerlings, P.; Faubel, M.; Winter, B.; Blumberger, J. *J. Phys. Chem. B* **2010**, *114*, 9173.

(49) Oberhofer, H.; Blumberger, J. *Angew. Chem., Int. Ed.* **2010**, *49*, 3631.

(50) Bernhard, P.; Helm, L.; Ludi, A.; Merbach, A. E. *J. Am. Chem. Soc.* **1985**, *107*, 312.

**Table 3.** Ranking of Protein Residues According to Their Contribution to Reorganization Free Energy for ET<sup>a</sup>

protein	rank	residue	$\lambda_r^b$ (meV)	$\langle d \rangle_A^c$ (Å)	$\Delta d^d$ (Å)	$\Delta \langle \Delta p^{\parallel} \rangle^e$ (D)
cca <sup>f</sup>	1	Glu104	380	7.5	1.9	0.2
	2	Lys22	210	12.3	-3.8	-6.1
ccb	1	Glu104	150	9.5	0.9	0.7
cb5b	1	Glu59	130	7.9	2.3	2.0
	2	Lys2	120	23.0	-2.4	-22.1
	3	Arg84	110	12.1	-1.7	-2.4

<sup>a</sup> Residues with a contribution larger than 0.1 eV are listed only.

<sup>b</sup> Permanent charge contribution of a residue to reorganization free energy.

<sup>c</sup> Average distance between center of mass of residue and the electron acceptor (Ru-complex) in the initial state A.

<sup>d</sup> Equation 10.

<sup>e</sup> Equation 11. <sup>f</sup> Average of trajectories 1 and 2.

In the following, we analyze the protein contribution to reorganization free energy. For this purpose, the protein reorganization free energy due to the fixed point charges is broken down into contributions from single amino acids. Residues with contributions larger than 0.1 eV are summarized in Table 3 and shown in Figure 7. In Table 3, we also give the distance between the center of mass of a protein residue and the Ru-complex in the initial ET state,  $\langle d \rangle_A$ . We find that all residues contributing significantly to reorganization free energy in cca, ccb, and cb5b have a charged side chain and are close to the Ru-complex, at a distance  $\langle d \rangle_A = 7\text{--}12$  Å (except Lys2 of cb5b, see below). Interestingly, there are no residues in the vicinity of the native heme cofactors that exhibit significant reorganization energy. In the designed 4-helix bundle protein, no single residue exhibits a reorganization free energy larger than 0.1 eV in agreement with our previous simulations.<sup>20</sup> The protein contribution is instead more evenly distributed over the residues.

The main molecular motions that give rise to protein reorganization free energy can be described by two geometrical parameters, (i) the change in distance between a protein residue and the Ru-complex in the initial (A) and final (B) ET state:

$$\Delta d = \langle d \rangle_B - \langle d \rangle_A \quad (10)$$

and (ii) the change in orientation of the projected dipole moment  $\Delta p^{\parallel}$  of a protein residue in states A and B:

$$\Delta \langle \Delta p^{\parallel} \rangle = \langle \Delta p^{\parallel} \rangle_B - \langle \Delta p^{\parallel} \rangle_A \quad (11)$$

$$\Delta p^{\parallel} = \vec{\mu}_r \cdot \vec{d}_2 / d_2 - \vec{\mu}_r \cdot \vec{d}_1 / d_1 \quad (12)$$

where  $\vec{\mu}_r$  is the dipole moment of residue  $r$  due to the fixed point charges, and  $\vec{d}_1 = \vec{d}_{\text{Ru}} - \vec{d}_r$ ,  $\vec{d}_2 = \vec{d}_{\text{Fe}} - \vec{d}_r$ ,  $d_i = |\vec{d}_i|$ , with  $\vec{d}_r$ ,  $\vec{d}_{\text{Ru}}$ , and  $\vec{d}_{\text{Fe}}$  the position vectors of the centers of mass of residue  $r$ , the Ru-complex, and the heme, respectively. For negatively (positively) charged residues such as Glu (Lys),  $\Delta d > 0$  ( $\Delta d < 0$ ) is correlated with a positive contribution to reorganization free energy due to change in distance. For residues of any charge,  $\Delta \langle \Delta p^{\parallel} \rangle < 0$  ( $\Delta \langle \Delta p^{\parallel} \rangle > 0$ ) is correlated with a positive (negative) contribution to reorganization free energy due to change in dipole orientation.  $\Delta d$  and  $\Delta \langle \Delta p^{\parallel} \rangle$  are summarized in Table 3.

In cca most of the protein reorganization free energy is due to terminal Glu104 and Lys22. In the initial ET state, shown in green in Figure 7A, the negatively charged terminal carboxylate group of Glu104 forms a hydrogen bond with the polar ammonia ligands of the Ru-complex. Upon electron injection into Ru<sup>3+</sup> (final state, shown in orange), the hydrogen bond breaks. Glu104

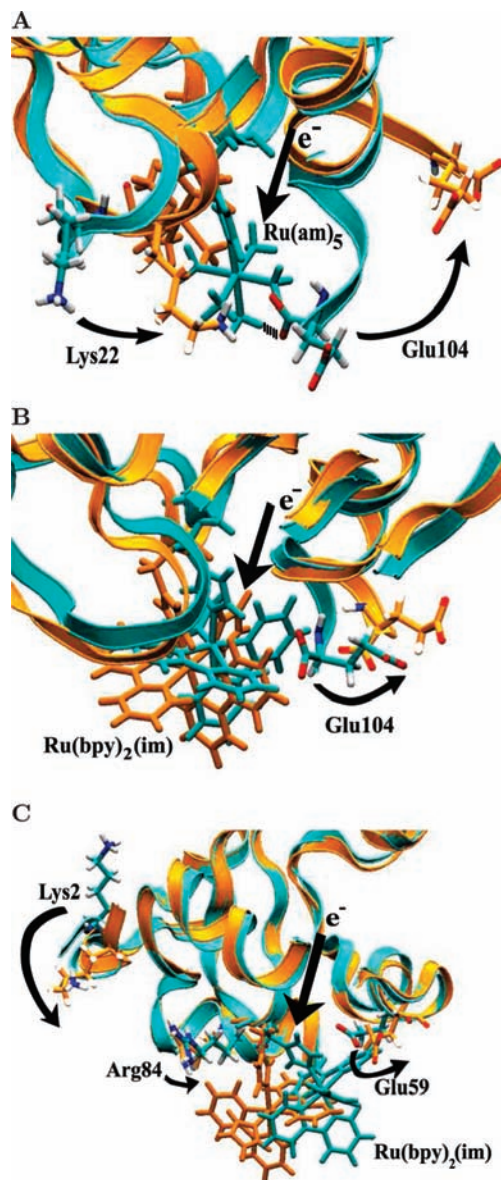


**Figure 7.** Analysis of the protein response to ET in cca (A), ccb (B), and cb5b (C). Two snapshots of the protein were selected randomly and aligned, one from a trajectory in the initial ET state (green) and one from a trajectory of the final ET state (orange). Protein residues that contribute more than 0.1 eV to the total reorganization free energy are depicted in stick representation. Arrows indicate injection of an electron into the Ru-complex and the subsequent response of the protein residues.

moves away from the Ru-complex ( $\Delta d > 0$ ) as a consequence of the repulsive interaction with the excess electron, and the positively charged side chain of Lys22 moves toward the Ru-complex ( $\Delta d < 0$ ). In ccb, Glu104 does not interact significantly with the hydrophobic Ru(bpy)<sub>2</sub>(im)His33 complex; see Figure 7B. Consequently, the response to electron injection is weaker than for cca, as is indicated by the smaller reorganization free energy contribution of this residue and the smaller change in  $\Delta d$ . No other residue in ccb contributes more than 0.1 eV to reorganization free energy. Analyzing the protein response in cb5b, we find a relatively large contribution for Lys2, even though this residue is 23 Å away from the donor and acceptor complexes. The long positively charged side chain of Lys2 effectively “tracks” the transfer of the electron (see Figure 7C). This leads to a particularly large change in the orientation of



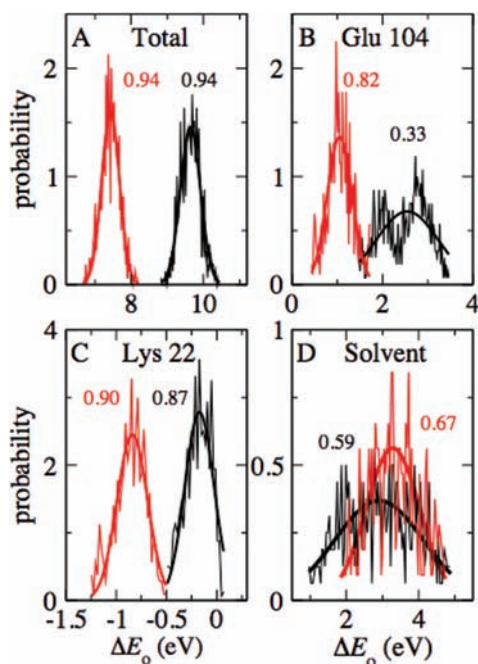


**Figure 8.** Probability distribution of the outer-sphere energy gap of cca (trajectory 1). The total outer-sphere distributions shown in panel (A) are identical to the ones shown in Figure 4A. Distributions of the permanent charge contribution of residues and the solvent to the outer-sphere energy gap are shown in panels (B)–(D). The distributions shown in black are for the initial state, and the ones shown in red are for the final state. Data points within two standard deviations of the average energy gap were collected in bins of width 0.02 eV (thin lines). Gaussian fit functions are shown in thick lines, and the corresponding correlation coefficients are indicated.

the dipole moment ( $\Delta\langle\Delta p^{\parallel}\rangle \ll 0$ ), and to a significant contribution to reorganization free energy.

Finally, we would like to point out that the energy gap fluctuations due to single amino acid residues and the solvent are in general non-Gaussian as opposed to the Gaussian nature of the total energy gap fluctuations. This is illustrated in Figure 8, where we show the total energy gap distribution and the contributions due to Glu104, Lys22, and the solvent for cca. Glu104 exhibits a bimodal distribution in the initial ET state of cca due to repeated formation and breaking of a hydrogen bond between the deprotonated terminal acid group of Glu104 and an ammonia ligand of the Ru-complex. Coupled to these events is the dynamics of hydrogen bonding between solvent water molecules and the ammonia ligands. The latter is also non-Gaussian. Given the large number of atoms contributing to the total energy gap fluctuations, the Gaussian statistics of the total gap in Figure 4 may be interpreted in terms of the central limit theorem. However, a key assumption of this theorem, that the individual distributions are uncorrelated, is clearly not fulfilled for protein solutions.

## 5. Concluding Remarks

To summarize, we have computed the reorganization free energy for four different heme containing electron transfer proteins using classical molecular dynamics simulation for the outer-sphere contribution and density functional calculations for the inner-sphere contribution. The values obtained for cca, ccb,

and cb5b are all very similar, 1.2–1.3 eV and within the empirical range of values assumed to apply to proteins where one oxidation site is exposed to water, 1.1–1.5 eV.<sup>7</sup> The computed value for the designed 4-helix bundle protein, 0.94 eV, is significantly smaller and at the upper end of reorganization free energies usually assumed to apply to ET proteins where both cofactors are excluded from the solvent, 0.6–0.9 eV.<sup>7</sup> Thus, our calculations on the four proteins lend support to these empirical guidelines for estimating reorganization free energy.

Nature has selected redox active cofactors for biological electron transport, which exhibit minimal reorganization free energy. The dominating part of the activation barrier for ET comes from the surrounding protein and solvent. The specific contributions of these two media to outer-sphere reorganization energy depend, among other factors, on the solvent accessibility and hydrophilicity of donor and acceptor groups, but also on their local interactions with nearby protein residues. The present analysis of the protein contributions in cca, ccb, and cb5b has shown that none of the residues in the vicinity of the native heme groups contribute significantly to reorganization free energy. The few residues that have a sizable contribution are located close to the synthetic Ru-complex at the surface of the protein, which is not present in the native system. This is also where most of the solvent reorganization occurs. Interestingly, because the reorganization free energy of ccb and cb5b is roughly the same, the different fold of the two proteins does not have a sizable effect.

The present characterization of reorganization energy has important implications for the engineering of artificial electron transport proteins.<sup>30</sup> Here, the driving force for ET should be small ( $-0.3 < \Delta A < 0$  eV), so as to minimize energy losses due to dissipation. This in turn requires small reorganization free energies for efficient transport, as the ET rate  $k_c$  in eq 1 approaches a maximum at  $\lambda = -\Delta A$ . Our simulations suggest that full exclusion of the redox active cofactors from the solvent is of principal importance to reach this aim. Indeed, by placing both redox active cofactors inside the scaffold of a designed 4-helix bundle protein,<sup>30</sup> we predict that reorganization free energy is significantly lowered relative to the proteins where one cofactor is solvent exposed. A further decrease could be achieved in this particular example by modifying the protein so that water molecules cannot penetrate the empty space between the two cofactors. Our simulations indicate that protein reorganization is more difficult to control because it typically involves a large number of residues, each contributing a small fraction.

**Acknowledgment.** The Royal Thai Government is acknowledged for a Ph.D. scholarship (V.T.), EPSRC is acknowledged for a First Grant (H.O., J.B.), and The Royal Society for a University Research Fellowship and a research grant (J.B.). We would further like to thank the High Performance Computing Facilities HECToR, Edinburgh, and the Center of Computational Chemistry, University of Cambridge, for computer time and assistance.

**Supporting Information Available:** Complete refs 29 and 32. This material is available free of charge via the Internet <http://pubs.acs.org>.

JA107876P